How to cite: *Angew. Chem. Int. Ed.* **2024**, *63*, e202401343
doi.org/10.1002/anie.202401343

Protein Structure

Including the Ensemble of Unstructured Conformations in the Analysis of Protein's Native State by High-Pressure NMR Spectroscopy

*Frederic Berner and Michael Kovermann**

Abstract: The analysis of pressure induced changes in the chemical shift of proteins allows statements on structural fluctuations proteins exhibit at ambient pressure. The inherent issue of separating general pressure effects from structural related effects on the pressure dependence of chemical shifts has so far been addressed by considering the characteristics of random coil peptides on increasing pressure. In this work, chemically and pressure denatured states of the cold shock protein B from *Bacillus subtilis* (*Bs*CspB) have been assigned in 2D ^{1}H-^{15}N HSQC NMR spectra and their dependence on increasing hydrostatic pressure has been evaluated. The pressure denatured polypeptide chain has been used to separate general from structural related effects on ^{1}H and ^{15}N chemical shifts of native *Bs*CspB and the implications on the interpretation of pressure induced changes in the chemical shift regarding the structure of *Bs*CspB are discussed. It has been found that the ensemble of unstructured conformations of *Bs*CspB shows different responses to increasing pressure than random coil peptides do. Thus, the approach used for considering the general effects that arise when hydrostatic pressure increases changes the structural conclusions that are drawn from high pressure NMR spectroscopic experiments that rely on the analysis of chemical shifts.

Introduction

The ability of proteins to adopt multiple conformations and to sample a broad range of structures within their energy landscape is tightly linked to their function in biochemical processes.[1] Therefore, it is crucial to gain knowledge on structural fluctuations proteins undergo to fully capture the mechanisms they are involved in. As proteins can be described as dynamic equilibria between a ground state and conformational ensembles belonging to high-energy substates sophisticated approaches enabling the investigation of these rather lowly populated high-energy states in terms of structure and thermodynamics are required. Here, the application of high pressure (HP) NMR spectroscopy represents a powerful approach to conduct such experiments at atomic resolution. It allows the determination of thermodynamic parameters such as changes in volume, ΔV, and compressibility, $\Delta\beta$, in a local as well as global manner yielding specific insights into the inherent flexibility of the protein under study.[2] Considering that an increase in hydrostatic pressure stabilizes conformations with a lower partial molar volume according to LeChatelier's principle and that the partial molar volume of a protein decreases with the loss of conformational order according to the "volume rule", perturbations of the energy landscape by applying hydrostatic pressure lead to a population of high-energy excited states that are invisible at ambient hydrostatic pressure.[3] Generally, high-resolution NMR spectroscopic experiments provide access to structural information by monitoring e.g. the NOE, ^{3}J coupling constants or numerical values for the chemical shift. Numerical values for chemical shifts are particularly useful parameters as they can be directly acquired and report on structural features with high reliability.[4] The impact of increasing hydrostatic pressure on the chemical shift comprising all NMR active nuclei can be experimentally assessed while ^{1}H and ^{15}N are the most frequently used representatives. Specifically, the impact of high hydrostatic pressure on chemical shift values of ^{1}H nuclei has been primarily linked to changes in the length of hydrogen bonds either to solvent molecules or intramolecularly.[5] The electric field effect and the magnetic anisotropy effect, contribute to the ^{1}H chemical shift of amide protons in hydrogen bonds with both shortening and straightening of hydrogen bonds resulting in downfield shifts in corresponding ^{1}H NMR spectra.[6] The chemical shift value of ^{15}N nuclei comprising backbone amides depends on a variety of parameters including the length of the hydrogen bonds they are involved in and backbone dihedral angles.[7] In terms of increasing hydrostatic pressure ^{15}N chemical shift values also tend to mainly downfield shifts. The same observation is made for shortening of associated hydrogen bonds and perturbations of backbone torsion angles.[8] When following the changes of chemical shift values comprising both ^{1}H and ^{15}N nuclei varying degrees of

[*] F. Berner, Prof. Dr. M. Kovermann
Department of Chemistry
University of Konstanz
Universitätsstrasse 10, 78464 Konstanz (Germany)
E-mail: michael.kovermann@uni-konstanz.de

linearity have been observed. Some proteins, e.g. hen lysozyme[9] or BPTI[5,8] show a high linearity in the change of chemical shift values upon an increase of hydrostatic pressure for almost all residues. In contrast, pronounced non-linearity is seen for other proteins such as HPr,[10] β-lactoglobulin[11] and the Rap1 A complex of RalGDS-RBD (RalCom) .[12] A linear change of the chemical shift value can be attributed to a linear change of corresponding structural parameters whereas it is supposed that the isothermal compressibility β_T is independent of high hydrostatic pressure present at a certain site. In fact, a linear change of chemical shift values originates from changes regarding the native state *N*.[8] The isothermal compressibility is related to volume fluctuations δV of a protein by

$$\langle(\delta V)^2\rangle = k_B T V \beta_T \quad (1)$$

where k_B is the Boltzmann constant, T is the absolute temperature and V is the partial volume of the protein.[13] Thus, fluctuations in volume do not change within the range of hydrostatic pressure in which linear changes of chemical shift values are observed.[14] In contrast, non-linear contributions to pressure-induced changes of chemical shift values indicate that β_T varies with hydrostatic pressure. It is supposed that non-linearity originates from a low-lying excited state *N'* which has a smaller partial molar volume than *N* and therefore becomes rather populated at increasing hydrostatic pressure.[14] The magnitude of linear and non-linear contributions to the changes in chemical shift values can be assessed by performing least-square fits of the equation

$$\delta_i(p) = a_i + b_i(p - p^0) + c_i(p - p^0)^2 \quad (2)$$

to the experimentally obtained chemical shift values. Here, δ_i is the chemical shift value of residue i, a_i is the chemical shift value at 1 bar, b_i (ppm/bar) is the linear coefficient, p (bar) represents the hydrostatic pressure, p^0 is the atmospheric pressure ($\approx$1 bar) and c_i (ppm/bar^2) is the non-linear coefficient.[11] The coefficients determined in this way can then be analyzed atom by atom comprising the protein under study.[6] The linear coefficients b_i are often interpreted as a measure of the magnitude of structural changes regarding *N*,[6] whereas the non-linear coefficients c_i report on low-lying excited states *N'* that may be linked to the hydration of water-accessible cavities in the protein.[11–12,14–15] The effect hydrostatic pressure has on chemical shift values of a protein is assumed to be composed of two contributions. First, an unspecific effect attributed to general modifications regarding the interaction with solvent molecules and, secondly, a rather specific effect depending on structural changes of the protein. In the case that they are independent of each other the effects are supposed to be additive.[16] The comparison with chemical shift values obtained for small random-coil peptides[17] represents a common approach to separate unspecific effects on chemical shift values characteristic for a given amino acid residue from structure-dependent effects. This approach has been expanded to HP NMR for $^1H^N$ nuclei using the model peptide GGXA[18] as well as for backbone ^{15}N,[19] $^1H^\alpha$, $^{13}C^\alpha$, $^{13}C'$[20] and side chain ^{13}C,[21] ^1H and ^{15}N[22] nuclei using the sequence Ac-GGXA-NH_2. Performing this correction, linear and non-linear coefficients are then interpreted for the protein under study as shown in several examples in the literature.[16,23] Even though model peptides are especially useful to estimate the dependence of the chemical shift value on hydrostatic pressure in random coil motives, the potential site-specific impact of adjacent residues composing the primary sequence of interest[17b] are neglected. This deficiency can be partly compensated by using correction factors introduced by Schwarzinger et *al.*,[24] as it has been done for the pressure dependence of side-chain ^1H and ^{15}N nuclei in the model peptide Ac-G-G-X-A-NH_2.[22] However, these parameters have been empirically derived and cannot comprehensively capture the features a specific polypeptide sequence inherently has. Another drawback of the model peptide approach is based on the fact that existing experimental conditions (e.g. pH value, buffer used, temperature, ionic strength) each have a precise impact on changes of chemical shift values which cannot be reliably predicted.[25] Here, we introduce a new approach to precisely differentiate between specific effects on chemical shift values that originate from structural changes within the protein under study and general effects caused by changes regarding interactions with the solvent. Experimental data have been acquired for the cold shock protein CspB from *Bacillus subtilis* (*Bs*CspB)[26] which has been frequently used as a model protein in numerous folding studies.[27] The folding-to-unfolding reaction follows a two-state mechanism with folding and unfolding rate constants on the millisecond timescale as revealed by stopped-flow fluorescence and NMR spectroscopy.[27d,f,g] Advantageously, the relatively low overall thermodynamic stability of *Bs*CspB ($\Delta G^0 = 8.9$ kJ/mol)[27e] allows the direct observation of the ensemble of unstructured conformations in two-dimensional heteronuclear ^1H-^{15}N HSQC NMR spectra at hydrostatic pressures within the range applicable with HP NMR spectroscopy. By subtracting the dependence of chemical shift values observed for the pressure unfolded polypeptide chain (present at native conditions) from corresponding changes in chemical shift values observed for the native state present at exact same conditions, changes in chemical shift values are obtained which, per se, solely stem from specific structural changes. Thus, the approach introduced here does not require the use of model peptides as the correction for general effects that accompany the change in hydrostatic pressure is made by using the same polypeptide sequence. Consequently, the corrected linear and non-linear coefficients then enable to reliably analyze the hydrogen bonding network, the compressibility and the role of cavities comprising *Bs*CspB in a site-specific manner.

Results and Discussion

Pressure-induced changes of chemical shifts have been quantified in the past by either determining linear and non-linear coefficients without any correction for unspecific

effects[10–12,15] or by subtracting coefficients obtained for short model peptides.[16,23b,c] In this work, a new approach using pressure-induced changes in chemical shift values of pressure denatured *Bs*CspB is introduced. All three approaches are highlighted in Scheme 1.

Due to its low overall thermodynamic stability *Bs*CspB is often used as a model protein in protein folding-to-unfolding studies as it is known to undergo a cooperative unfolding transition upon adding denaturing agents[27d,e] or increasing temperature.[27b] Here, the folding-to-unfolding transition of *Bs*CspB as induced by increasing hydrostatic pressure was, first, probed by recording one-dimensional ^{1}H NMR spectra using a range of hydrostatic pressure between 1 and 3000 bar (Figure 1A). A monotonic increase in signal height of resonance signals of aliphatic protons comprising both the native state and unfolded conformers and a parallel decrease in signal height of resonance signals reporting exclusively on the native state of *Bs*CspB is observed. Determining the fraction of the native state of *Bs*CspB, f_N, enables then the determination of thermodynamic parameters quantifying the folding-to-unfolding transition (Figure 1B). Fitting eq. S1 to the experimental data reports on the difference in free energy, $\Delta G^0 = 8.6 \pm 0.2$ kJ/mol, and the difference in volume between N and U, $\Delta V^0 = -43.0 \pm 0.1$ mL/mol. Consequently, about 83 % of *Bs*CspB molecules populate the ensemble of unstructured conformations at a

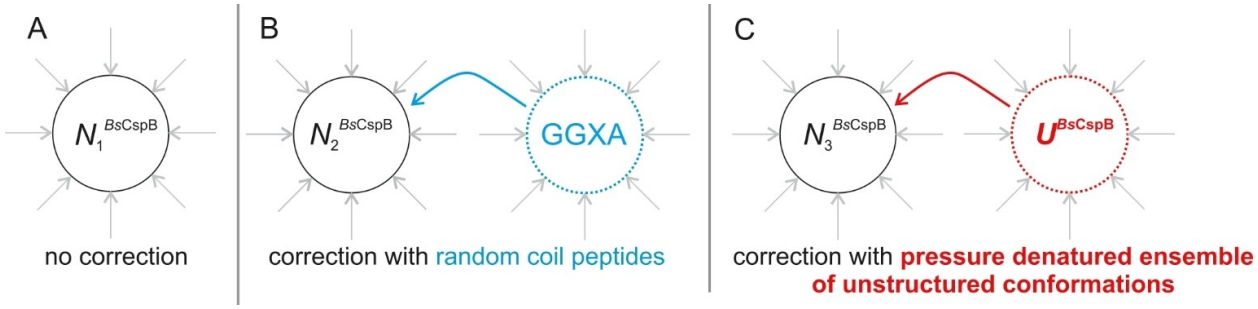

Scheme 1. Impact of hydrostatic pressure on structural properties of native *Bs*CspB, *N*, dependent on experimental strategy pursued. (A) Structural properties of native *Bs*CspB are analyzed by experimental data exclusively acquired for *Bs*CspB, no correction applied. (B) Structural properties of native *Bs*CspB are analyzed by experimental data acquired for both *Bs*CspB and random coil peptides comprising the motif GGXA. A correction is applied by subtracting the parameters obtained for GGXA from parameters acquired for *Bs*CspB according to (A). (C) Structural properties of native *Bs*CspB are analyzed by experimental data acquired for both *Bs*CspB and the pressure denatured ensemble of unstructured conformations of *Bs*CspB that is present under native conditions (U^{BsCspB}). A correction is applied by subtracting the parameters obtained for U^{BsCspB} from parameters acquired for *Bs*CspB according to (A). The experimental work outlined in the present manuscript focuses on the characterization of native *Bs*CspB dependent on data treatment resulting in N_1, N_2 and N_3. The application of hydrostatic pressure on the molecule under study (encompassed by a circle; continuous line for native *Bs*CspB as dashed line for the molecule used for correction) is highlighted by arrows colored in grey.

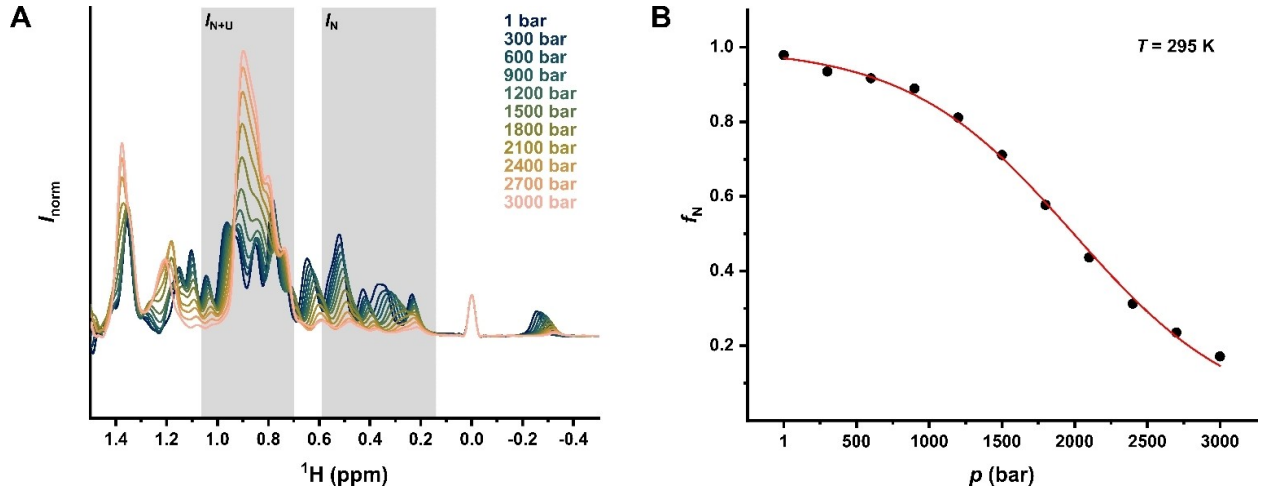

Figure 1. Increasing hydrostatic pressure leads to unfolding of native *Bs*CspB. Chemical shifts reporting on aliphatic resonance signals observed in a series of one-dimensional ^{1}H NMR spectra of *Bs*CspB using hydrostatic pressure in a range between 1 and 3000 bar. Spectral regions used for integration corresponding to either native (I_N) or native + ensemble of unstructured conformations (I_{N+U}) are subsequently used for the calculation of the fraction native (f_N) and are highlighted by using a background colored in grey. All spectra have been referenced using the resonance signal originating from TMSP arising at 0 ppm. (B) Values for f_N determined using the NMR spectra shown in A and plotted dependent on hydrostatic pressure applied (filled circles, colored in black). Applying a two-state model for the folding-to-unfolding transition enables to obtain thermodynamic parameters for the transition and the corresponding fitting function is shown in red color. The data have been acquired at $B_0 = 14.1$ T and $T = 295$ K by using $c^{BsCspB} = 50$ μM.

hydrostatic pressure of 3000 bar (compared to about 2 % at a hydrostatic pressure of 1 bar) which makes it possible to directly observe values of chemical shifts reporting on the ensemble of unstructured conformations in two-dimensional ^{1}H-^{15}N HSQC NMR spectra. This set of experimental data has been acquired and is presented next.

Structural changes regarding the native state as well as low-lying excited states of the protein under study can be detected by applying HP NMR spectroscopy and analyzing corresponding changes in chemical shifts observed in two-dimensional ^{1}H-^{15}N HSQC NMR spectra.[6] Thus, 2D ^{1}H-^{15}N HSQC NMR spectra have been acquired for *Bs*CspB at hydrostatic pressures in the range between 1 and 3000 bar (Figure 2). Most of the cross-peaks arising in 2D ^{1}H-^{15}N HSQC NMR spectra experience shifts in down-field direction in ^{1}H and ^{15}N dimensions as expected for a compression of the native state.[5,8] However, the cross-peaks shift non-uniformly indicating that a homogeneous compression is not the only process present that contributes to changes in chemical shifts. Additionally, as the increase in hydrostatic pressure induces unfolding of *Bs*CspB, cross-peaks corresponding to the ensemble of unstructured conformations arise at about $^{1}\mathrm{H} \simeq 8.3$ ppm as the ensemble of unstructured conformations becomes significantly populated. Here, a noticeable trend in the ^{1}H-^{15}N HSQC spectra displayed in Figure 2 was found. Resonance signals corresponding to glycine residues sensing the ensemble of unstructured conformations found in the range between 109 and 112 ppm in the ^{15}N dimension shift non-uniformly with increasing hydrostatic pressure (Figure 3A). This is somewhat unexpected as the absence of any secondary or tertiary structure shall go along with a comparable dependence on hydrostatic pressure of cross-peaks analyzed. Thus, we aimed to get comprehensive site-specific information on the pressure dependence of chemical shift values that correspond to the ensemble of unstructured conformations of *Bs*CspB in the presence of $c^{\mathrm{urea}} = 6$ M.[27b,d,e] In total, 52 out of 67 residues comprising *Bs*CspB have been assigned (Figure S1). Subsequently, a series of 2D ^{1}H-^{15}N HSQC spectra have been acquired using the same range of hydrostatic pressure used for native state conditions (Figure S2). Note that again resonance signals corresponding to glycine residues found in the range between 109 and 112 ppm in the ^{15}N dimension shift non-uniformly (Figure 3C). Then linear and non-linear coefficients of chemical shift values of both ^{1}H and ^{15}N dimensions have been determined and corresponding results are shown in Figure S3. The ensemble of unstructured conformations of *Bs*CspB as present at $c^{\mathrm{urea}} = 6$ M shows an attenuated dependence on hydrostatic pressure compared to native *Bs*CspB (shown in more detail below), as observed for hen lysozyme before.[15] When comparing the coefficients obtained for chemically denatured *Bs*CspB with the coefficients obtained for the random coil peptide Ac-GGXA,[19] exemplary shown for linear coefficients in the ^{1}H dimension (Figure 3D), significant deviations are found. Interestingly, a similar result has been found in a study investigating the impact of hydrostatic pressure on the intrinsically disordered protein α-synuclein for non-linear ^{1}H coefficients.[28] The assignment of cross-peaks of chemically denatured *Bs*CspB cannot be directly transferred to pressure denatured *Bs*CspB as the presence of urea impacts the values of chemical shifts significantly. In other words, changes of chemical shift values of chemically denatured *Bs*CspB induced by changes in hydrostatic pressure are also impacted by the presence of

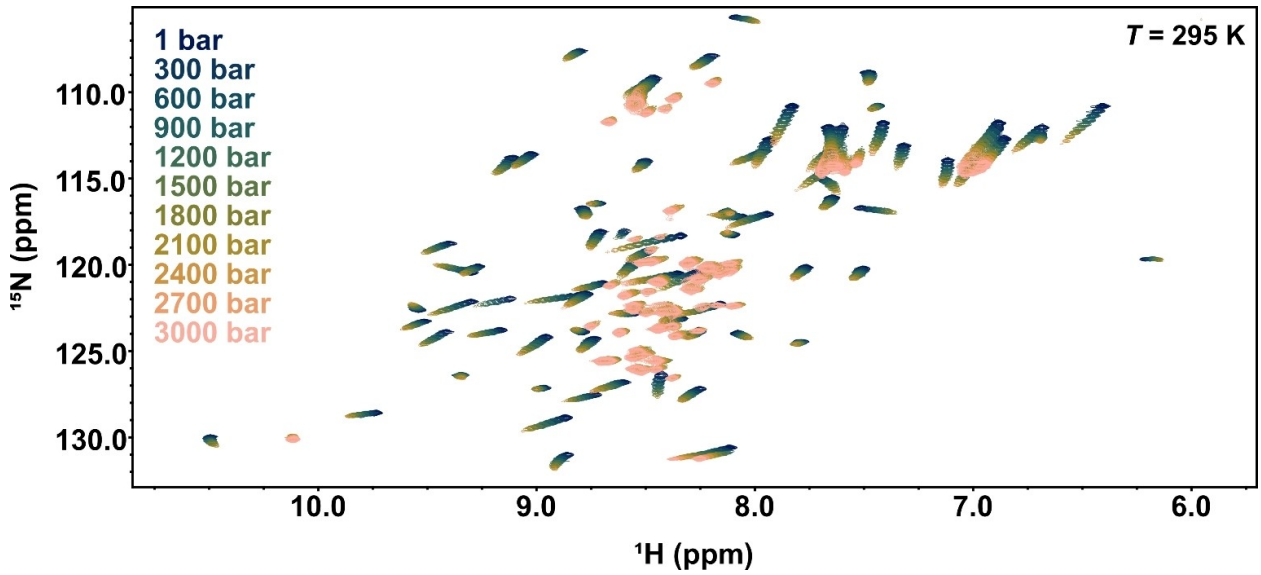

Figure 2. Unfolding of native *Bs*CspB by increasing hydrostatic pressure as observed in two-dimensional ^{1}H-^{15}N HSQC NMR spectra. Increasing the hydrostatic pressure from 1 to 3000 bar induces a significant increase of the population reporting on the ensemble of unstructured conformations at about $^{1}\mathrm{H} \simeq 8.3$ ppm whereas the signal heights of dispersed cross-peaks that report on the native state of *Bs*CspB decrease. The data have been acquired at $B_0 = 14.1$ T and $T = 295$ K by using $c^{\mathrm{BsCspB}} = 50$ μM. Linear and non-linear components obtained by analyzing the changes in chemical shifts are shown in Figures 4 and S4–S6. All 2D NMR spectra shown in this Figure have been directly referenced using TMSP in the ^{1}H and indirectly in the ^{15}N dimension, respectively. Assigned spectra of native and pressure denatured *Bs*CspB are shown in Figures S7 and S8.

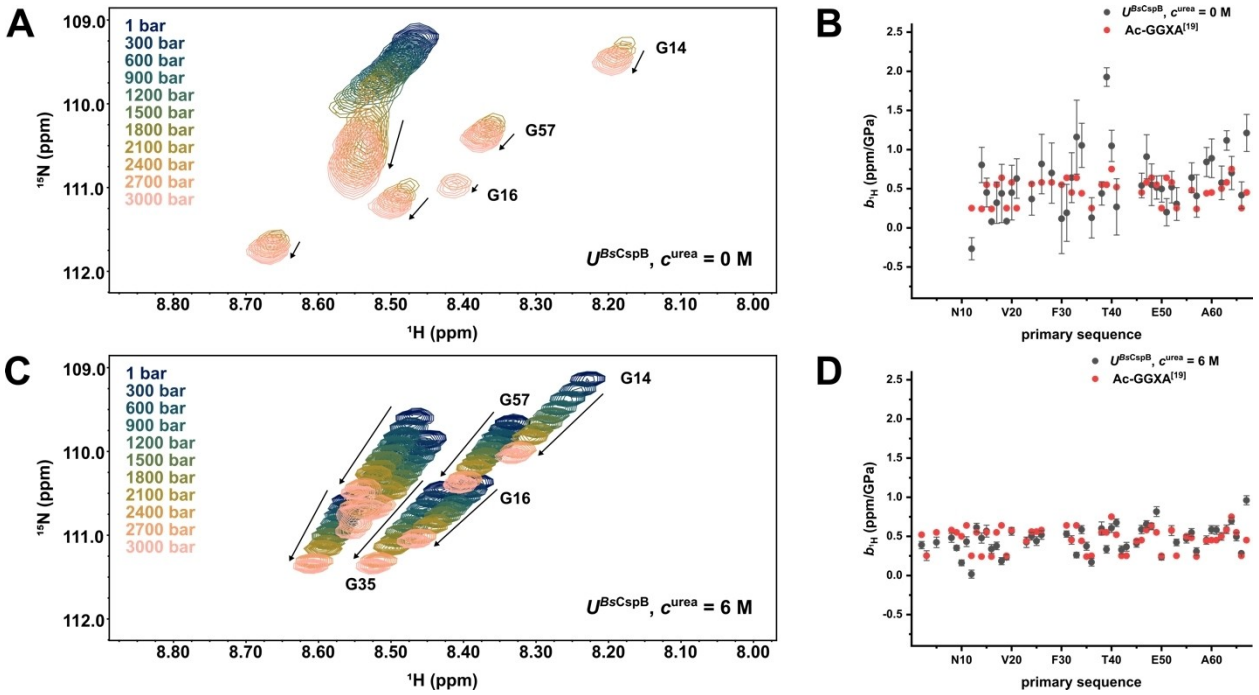

Figure 3. Characterization of the ensemble of unstructured conformations of *Bs*CspB, U^{BsCspB}. (A) Spectral area characteristic for glycine residues in ^{1}H-^{15}N HSQC NMR spectra acquired in a range between 1 and 3000 bar comprising *Bs*CspB at $c^{urea}=0$ M urea. (B) Comparison of linear ^{1}H coefficients obtained for signals corresponding to pressure denatured *Bs*CspB (black) and the random coil peptide Ac-GGXA[19] (red). (C) Spectral area characteristic for glycine residues in ^{1}H-^{15}N HSQC spectra in a range between 1 and 3000 bar for *Bs*CspB at $c^{urea}=6$ M. (D) Comparison of linear ^{1}H coefficients obtained for signals corresponding to chemically denatured *Bs*CspB (black) and the random coil peptide Ac-GGXA[19] (red). Residue-specific trajectories of chemical shift values leading to the data shown in panel B and D are found in Figure S14 (U^{BsCspB}, $c^{urea}=0$ M) and Figure S16 (U^{BsCspB}, $c^{urea}=6$ M).

urea. To investigate how chemical shift values of pressure denatured *Bs*CspB change with hydrostatic pressure, triple resonance experiments have been conducted at $p=3000$ bar to assign pressure denatured *Bs*CspB. Note that $c^{urea}=1$ M has been added to completely suppress any signals corresponding to native *Bs*CspB. These experimental conditions enabled to transfer assignments of resonance signals to NMR spectra recorded in absence of urea (Figure 2). In total, 45 out of 65 residues of pressure denatured *Bs*CspB have been assigned (Figure S8). Then, the trajectories of the chemical shifts have been followed in a range between 1200 and 3000 bar enabling the determination of linear and non-linear coefficients. These trajectories could be unambiguously followed for 39 out of the 45 assigned residues (for 22 residues within $1200\leq p\leq 3000$ bar, for 17 residues within $1500\leq p\leq 3000$ bar), corresponding results are shown in Figure S9. Again, a comparison of coefficients obtained for pressure denatured *Bs*CspB with coefficients obtained for the peptide Ac-GGXA,[19] exemplary shown for linear coefficients in the ^{1}H dimension in Figure 3B, shows that the numerical values are deviating considerably. Interestingly, comparing linear and non-linear coefficients for residues of the same type that reside at different positions in the primary sequence leads to numerical values that significantly differ as exemplarily shown for four alanine residues comprising *Bs*CspB in Table 1, also in comparison to numerical values obtained for Ac-GGXA.[19]

Thus, the numerical values determined strongly depend on the position in the primary sequence. The same trend for alanine residues can be observed when the chemically

Table 1: Linear and non-linear coefficients determined for alanine residues comprising pressure denatured *Bs*CspB. The linear and non-linear coefficients have been determined for all alanine residues sensing the ensemble of unstructured conformations constituting the primary sequence of *Bs*CspB at $c^{urea}=0$ M in the ^{1}H and the ^{15}N dimensions, respectively. Corresponding spectral data are shown in Figure 2. *data for model peptide has been taken from Koehler et *al.*, 2012.[19]

	S31-**A32**-I33	Q45-**A46**-V47	Q59-**A60**-A61	E66-**A67**	G-**A**-A* (peptide)
b_{1H} (ppm/GPa)	0.64 ± 0.32	0.54 ± 0.16	0.89 ± 0.25	1.21 ± 0.24	0.45 ± 0.02
b_{15N} (ppm/GPa)	1.55 ± 1.38	5.13 ± 1.58	3.00 ± 1.40	3.34 ± 0.56	2.74 ± 0.03
c_{1H} (ppm/GPa^2)	0.71 ± 0.71	0.30 ± 0.36	1.19 ± 0.57	1.32 ± 0.55	0.15 ± 0.08
c_{15N} (ppm/GPa^2)	0.11 ± 3.06	7.94 ± 3.64	2.36 ± 3.22	4.02 ± 1.30	1.49 ± 0.16

denatured ensemble of unstructured conformations of *Bs*CspB is analyzed within the range between 1 and 3000 bar of hydrostatic pressure (Table S1). The chemical shift index (CSI) for $^{13}C^{\alpha}$ nuclei has also been determined[29] to exclude the potential presence of residual structural motifs comprising pressure or chemically denatured *Bs*CspB. No hints of potential residual structural motifs have been found (Figures S10 and S11). Thus, we conclude that the position and thereby the structural embedding in the primary sequence impact the dependence of $^{1}H^{N}$ and backbone ^{15}N chemical shift values on hydrostatic pressure significantly. The corrections made so far in the field of HP NMR relying on spectroscopic information obtained for random coil peptides do not fully account for the local environment the amino acid residues sense. Consequently, we suggest an internal correction of *b* and *c* coefficients using spectroscopic information obtained for the ensemble of unstructured conformations to consider inherent structural features of the polypeptide chain under study in a comprehensive manner.

To evaluate the three approaches for determining pressure induced chemical shift coefficients (Scheme 1) we interpreted the coefficients by using the three-dimensional structure of native *Bs*CspB (1NMG) .[26b] A positive *b* value seen in the ^{1}H dimension is caused by a down-field shift of the respective cross-peak in corresponding ^{1}H-^{15}N HSQC spectra with increasing hydrostatic pressure which has been linked to a shortening of the corresponding hydrogen bond, either to the solvent or intramolecularly, the amide proton is involved in.[5] Consequently, a negative *b* value seen in the ^{1}H dimension may be interpreted as an elongation of the hydrogen bond the amide proton is a part of. The magnitude of the linear ^{1}H coefficients may then indicate how much the hydrogen bonds change in length (Figure 5A). On the other hand, the interpretation of non-linear ^{1}H coefficients is less straight-forward, with large absolute values being linked to structural transitions involving a low-lying excited state *N*' and the hydration of solvent-excluded cavities.[14] The pressure dependence of ^{15}N chemical shifts, however, is poorly understood and the coefficients cannot be easily interpreted in a structural manner.[28] For a structural interpretation of the coefficients obtained for *Bs*CspB we therefore focused on linear coefficients determined for the ^{1}H dimension as they are supposed to provide a rather direct structural readout. Non-linear ^{1}H and linear as well as non-linear ^{15}N coefficients are shown in Figures S4–S6. The linear ^{1}H coefficients determined for native *Bs*CspB are shown as a function of the primary sequence for the three approaches — applying no correction, applying correction using coefficients obtained from random coil peptides and applying a correction using coefficients of pressure denatured *Bs*CspB — in Figure 4. Means have been calculated and residues deviating by ±1 standard deviations from the mean are highlighted in light red and light blue, respectively. Residues deviating by ±2 standard deviations from the mean are highlighted in red and blue, respectively. This strategy enables the identification of key residues that are significantly impacted by increasing hydrostatic pressure. For these key residues we investigated whether they are involved in intramolecular hydrogen bonds either by using the pymol[30] prediction tool for showing polar contacts or by information provided by Garcia-Mira et *al.*[27a] For the case that residues are part of intramolecular hydrogen bonds these contacts are highlighted, again for all three approaches, in the structure of *Bs*CspB colored correspondingly to the magnitude of the associated linear ^{1}H coefficient (Figure 5B–D). In this way it becomes possible to directly identify intramolecular hydrogen bonds that are significantly shortened or elongated upon an increase of hydrostatic pressure according to underlying linear ^{1}H coefficients.

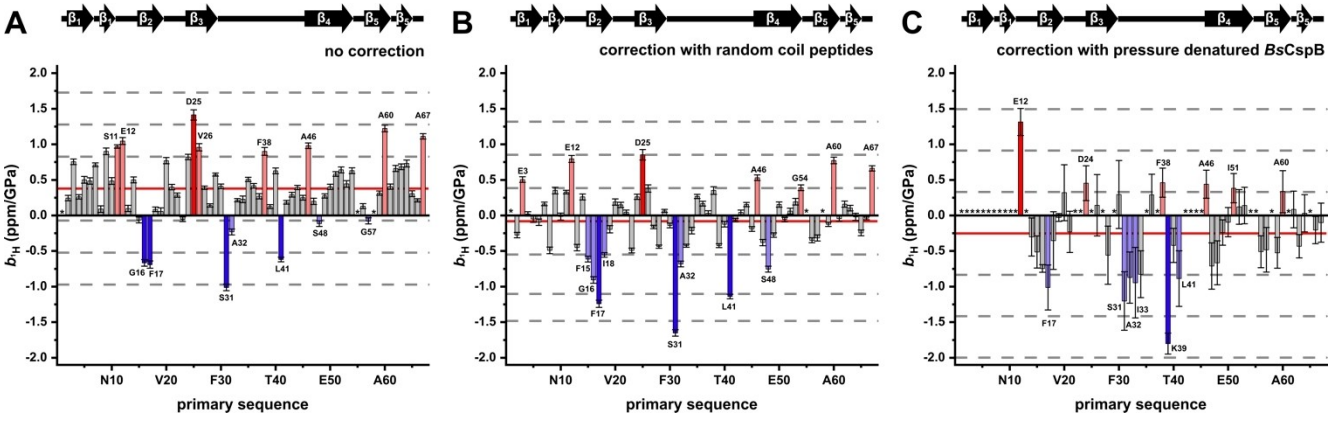

Figure 4. Linear coefficients in the ^{1}H dimension obtained for chemical shifts arising in two-dimensional ^{1}H-^{15}N HSQC NMR spectra acquired for native *Bs*CspB dependent on hydrostatic pressure. The horizontal lines indicate the mean *b* (continuous mode, red) and the mean ± standard deviation(s) (dotted mode, grey). Residues deviating by more than ±1 standard deviation from the mean are highlighted in light red/light blue and residues deviating by more than ±2 standard deviations from the mean are highlighted in red/blue. Coefficients were determined (A) with no correction applied (data of corresponding chemical shift values are shown in Figure S12), (B) using spectroscopic information obtained from random coil peptides for correction and (C) using spectroscopic information obtained from pressure denatured *Bs*CspB (U^{BsCspB}, $c^{urea} = 0$ M) for correction (data of corresponding chemical shift values are shown in Figures S12, S14). Residues (in either the native state or the ensemble of unstructured conformations) for which the values of chemical shifts could not be unambiguously followed in a pressure dependent manner are marked with an asterisk (*).

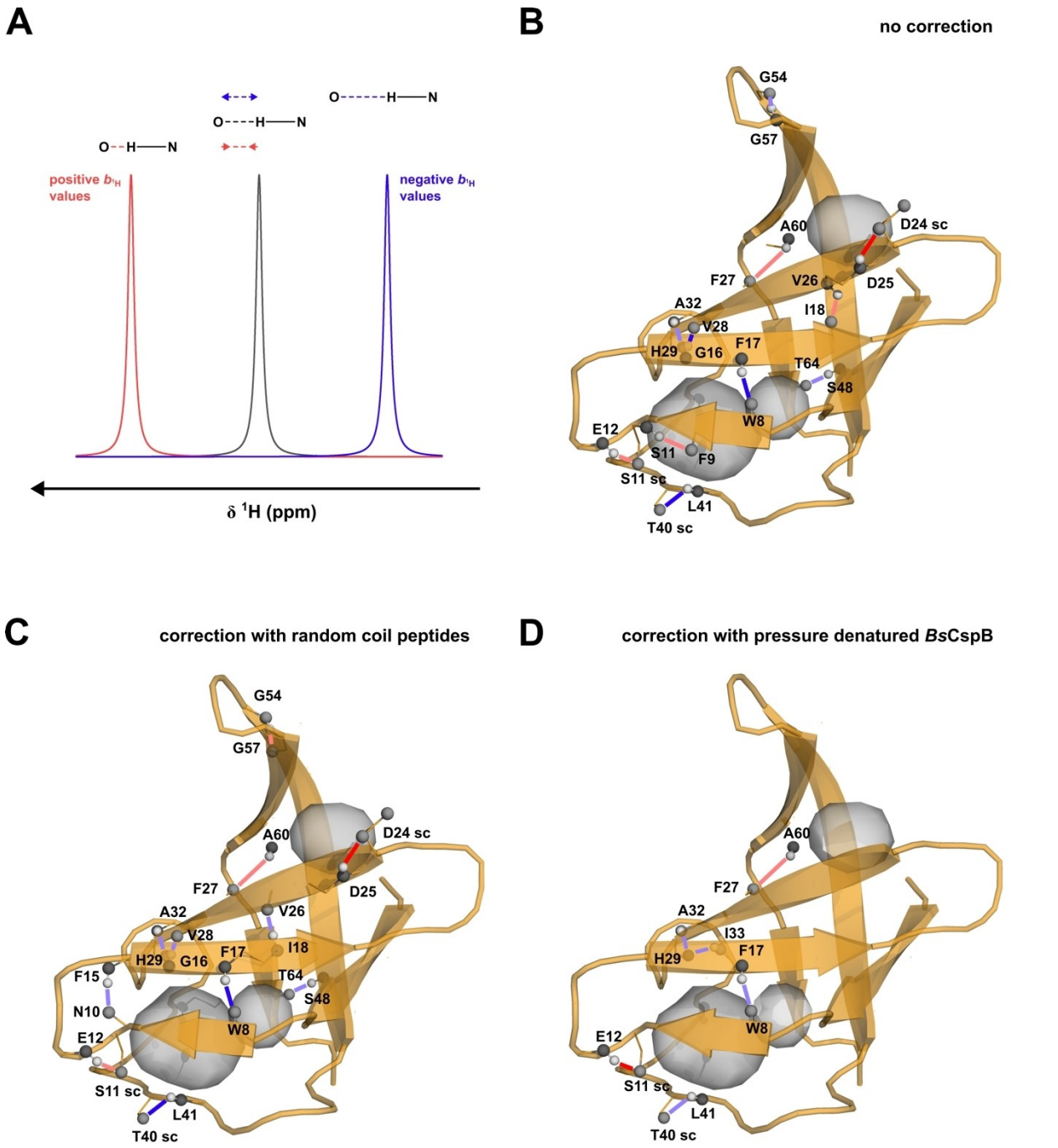

Figure 5. Relation between change in hydrogen bonding network comprising *Bs*CspB and the approach used for correction of general effects caused by an increase of hydrostatic pressure. (A) Schematic representation interpreting up-field and down-field shifts in the ^{1}H dimension and corresponding consequences for the length of a hydrogen bond. (B)–(D) Structural representations of *Bs*CspB (pdb: 1NMG).[26b] Atoms relevant for hydrogen bonds possessing linear ^{1}H coefficients that significantly deviate from the respective mean are shown as spheres with nitrogen atoms colored in dark grey, hydrogen atoms colored in almost white and oxygen atoms colored in light grey. Cavities as predicted by pymol[30] using a cavity detection radius of three solvent radii are shown in surface mode colored in grey. Hydrogen bonds are highlighted using straight lines colored corresponding to the linear ^{1}H coefficient associated with the respective amide proton. Structural representations are shown for all three approaches introduced here to determine the coefficients: (B) no correction, (C) correction using spectroscopic information obtained from random coil peptides and (D) correction using spectroscopic information obtained from the pressure denatured ensemble of unstructured conformation of *Bs*CspB (U^{BsCspB}, $c^{urea} = 0$ M).

Interestingly, comparable residues show conspicuous behavior across the three approaches. Thus, residues F17, S31, A32 and L41 show significantly deviated negative *b* values indicating an elongation of the respective hydrogen bonds. These residues also show small negative or positive temperature coefficients as determined recently[27b] suggesting that

they are indeed involved in hydrogen bonding.[31] Residue F17 (and G16) are located within the β_2 strand and form hydrogen bonds to V28 in the β_3 strand and W8 in the β_1 strand, thereby connecting the three strands.[27a] Residues S31, A32 and L41 are located within the loop connecting β_2 and β_3 strands. The amide proton of S31 is not supposed to be in an intramolecular hydrogen bond according to pymol[30] or Garcia-Mira et *al.*[27a] but exhibits a large positive temperature coefficient which suggests that it is indeed hydrogen bonded and L41 forms a hydrogen bond to the sidechain of T40 while the amide proton of A32 forms a hydrogen bond to H29.[27a]

These elongated hydrogen bonds are all accompanied by conspicuously pronounced non-linear coefficients (Figure S5) and envelop a relatively large cavity within the protein structure also depicted in Figure 5B–D. This property of the linear ^{1}H coefficients is conserved for all three approaches presented and indicates that this cavity might "break open" and is thus hydrated upon increasing hydrostatic pressure. The amide proton of D25, on the other hand, forms a hydrogen bond to the side chain of D24 which is considerably shortened at high hydrostatic pressure. Similarly, hydrogen bonds formed by A60 to F27 is also shortened. Intriguingly, these hydrogen bonds are all enveloping another cavity, one that seemingly gets compressed upon increasing pressure. Again, this key observation is more or less conserved for all three approaches. Even though the approaches lead to similar structural interpretations based on key residues strongly deviating from the mean, distinct differences can also be observed. While E12 which is involved in an intramolecular hydrogen bond shows a positive linear ^{1}H coefficient for all approaches, this property is significantly pronounced when pressure denatured *Bs*CspB is used to correct for unspecific effects as the corresponding resonance signal experiences an up-field shift in the ^{1}H-^{15}N HSQC NMR spectra. The hydrogen bonds of residues F15 to N10 and I18 to V26 — thereby also connecting the first three β strands of the β barrel structure and enveloping a cavity which is supposed to be hydrated at higher hydrostatic pressure — show a more pronounced elongation when their coefficients are corrected with random coil peptides or — to less extent — the unfolded polypeptide chain. Thus, the data acquired in our study suggest that residues that show peculiarity regarding features in hydrogen bonding are residing with considerable probability next to a cavity the three-dimensional fold of *Bs*CspB provides. We note, however, that the number of residues for which chemical shift values can be unambiguously determined for the ensemble of unstructured conformations is intrinsically limited due to spectral features *Bs*CspB possesses (Figure S8). Several residues are only observed to have a significant pressure response when a certain approach for correction is used, e.g. residue G57 which is only prominent when no correction is applied or residue G54 which only stands out when the coefficients are corrected using information obtained from random coil peptides. The hydrogen bond of I33 to H29 — next to the hydrogen bond of A32 to H29 enveloping the same cavity — is only found to be significantly elongated when its coefficient is corrected with its corresponding coefficient obtained for the ensemble of unstructured conformations. Also, residue K39 is conspicuous in the b_{1H} value when this correction is applied even though this residue does not contribute to the intramolecular network of hydrogen bonds comprising *Bs*CspB. The C-terminal residue A67 shows a pronounced linear ^{1}H coefficient when no or a correction using random coil peptides is applied. In contrast, no structural response is seen when the coefficient of the corresponding non-structured polypeptide chain is used for correction which appears convincing as the C-terminus comprising *Bs*CspB is not involved in secondary or tertiary structure. In summary, focusing on linear ^{1}H coefficients and key residues significantly deviating from the mean, the three approaches shown in Scheme 1 lead to an overall similar structural conclusion — in this case the "breaking" of one cavity comprising *Bs*CspB and the compression of another one. However, analyzing the coefficients in a more detailed — rather local — manner reveals that further residues comprising *Bs*CspB and their inherent intramolecular hydrogen bonding network have to be taken into account when different methods for correcting unspecific effects regarding hydrostatic pressure are used. In addition, the results found here may also pave the way to elucidate the folding-to-unfolding pathway of *Bs*CspB on a residue-by-residue manner when hydrostatic pressure is the experimental determinant. We are aware that wild type *Bs*CspB represents a rather special case by having the intrinsic advantage of probing *N* and *U* separately in a broad range of hydrostatic pressure due to low overall thermodynamic stability and possessing exchange rate constants enabling the work conducted. However, biochemical strategies are available (e.g. by applying site-directed mutagenesis) to tune the energy landscape of other proteins of interest such that they also become suitable to exclusively probe chemical shift values reporting on *U* that can then be used to correct chemical shift values that have been found for the native state while increasing hydrostatic pressure.

Conclusions

HP NMR spectroscopy is a powerful tool to investigate proteins in a structural manner and is supposed to illuminate conformational fluctuations proteins undergo at ambient conditions by populating conformers with a lower partial molar volume. The analysis of pressure induced changes in chemical shift values observed for the protein under study thereby represents one established method, often using linear and non-linear coefficients enabling structural conclusions. However, the dependence of chemical shift values of proteins on hydrostatic pressure is not only affected by structural transitions but also by a general effect attributed to the fact that solvent properties and the interaction of solvent molecules with the nuclei under investigation are changing when hydrostatic pressure increases. Thus, it is therefore necessary to precisely differentiate between these two effects which has so far been done by subtracting coefficients obtained for tetrapeptides of the type GGXA

which are not able to adopt any secondary or tertiary structure. Even though this approach captures effects that are not related to structural transitions it still has drawbacks. It does neither consider the influence neighboring residues have on the chemical shift values nor how different buffer conditions or changes in temperature may impact pressure induced changes in chemical shift values. In this work, we have introduced an approach circumventing these obstacles while acquiring a comprehensive set of NMR spectroscopic data on *Bs*CspB. The dependence of both the chemically and pressure denatured ensembles of unstructured conformations of *Bs*CspB on hydrostatic pressure shows that residues of the same type show different responses to hydrostatic pressure depending on their position in the primary sequence, also deviating from expected values based on random coil peptides. The changes in chemical shifts of the solely pressure denatured ensemble of unstructured conformations of *Bs*CspB report on effects that are not related to the secondary or tertiary structure of *Bs*CspB. In fact, the nuclei comprising the pressure denatured ensemble of the polypeptide chain sense the same proximity as in the native state, thereby excluding any effects originating from changing solvent interactions. Subsequently, we determined linear and non-linear coefficients for native *Bs*CspB using three different approaches. First, applying no correction, secondly, applying a correction using coefficients obtained for the peptide Ac-GGXA, and, thirdly, applying a correction using coefficients obtained for analyzing the ensemble of unstructured conformations of the same polypeptide chain. As linear ^{1}H coefficients provide a direct structural readout, we analyzed the coefficients regarding the three-dimensional structure of *Bs*CspB. We found that conclusions can be made based on the analysis of linear ^{1}H coefficients, e.g. which cavities in the protein are hydrated or compressed upon increasing hydrostatic pressure. The same key residues could be identified using the three approaches. However, in a more detailed analysis, significant differences in the structural interpretation arise such that the coefficients of particular residues possess a significant dependency on the approach used for the correction considering unspecific effects. This highlights the importance of considering an appropriate correction when pressure related coefficients are structurally interpreted in a quantitative manner. We suggest to conduct more research in this direction e.g. by computational approaches as well as further NMR spectroscopic experiments to work on the general effects that accompany an increase in hydrostatic pressure. However, the correction of coefficients that are used to report on structural features of the native state of a protein by using the coefficients obtained for the corresponding pressure denatured ensemble of conformations as introduced here provides a new approach to the analysis of pressure induced changes in chemical shifts of proteins.

Supporting Information

The authors have cited additional references within the Supporting Information (Ref. [32]).

Acknowledgements

We thank Tom Palmer and Vilson Karaj for support in data acquisition. We thank Hans Robert Kalbitzer for fruitful discussion and the University of Konstanz for the constant investment into the NMR infrastructure. Open Access funding enabled and organized by Projekt DEAL.

Conflict of Interest

The authors declare no conflict of interest.

Data Availability Statement

The data that support the findings of this study are available from the corresponding author upon reasonable request.

Keywords: NMR spectroscopy · protein folding · high-pressure chemistry · protein structures · solvent effects

[1] M. Kovermann, P. Rogne, M. Wolf-Watz, *Q. Rev. Biophys.* **2016**, *49*, e6.
[2] K. Akasaka, *Subcell. Biochem.* **2015**, *72*, 707–721.
[3] R. Kitahara, H. Yamada, K. Akasaka, P. E. Wright, *J. Mol. Biol.* **2002**, *320*, 311–319.
[4] T. Asakura, K. Taoka, M. Demura, M. P. Williamson, *J. Biomol. NMR* **1995**, *6*, 227–236.
[5] H. Li, H. Yamada, K. Akasaka, *Biochemistry* **1998**, *37*, 1167–1173.
[6] R. Kitahara, K. Hata, H. Li, M. P. Williamson, K. Akasaka, *Prog. Nucl. Magn. Reson. Spectrosc.* **2013**, *71*, 35–58.
[7] a) H. Le, E. Oldfield, *J. Biomol. NMR* **1994**, *4*, 341–348; b) X.-P. Xu, D. A. Case, *Biopolymers* **2002**, *65*, 408–423.
[8] K. Akasaka, H. Li, H. Yamada, R. Li, T. Thoresen, C. K. Woodward, *Protein Sci.* **1999**, *8*, 1946–1953.
[9] K. Akasaka, T. Tezuka, H. Yamada, *J. Mol. Biol.* **1997**, *271*, 671–678.
[10] H. R. Kalbitzer, A. Görler, H. Li, P. V. Dubovskii, W. Hengstenberg, C. Kowolik, H. Yamada, K. Akasaka, *Protein Sci.* **2000**, *9*, 693–703.
[11] K. Kuwata, H. Li, H. Yamada, C. A. Batt, Y. Goto, K. Akasaka, *J. Mol. Biol.* **2001**, *305*, 1073–1083.
[12] K. Inoue, T. Maurer, H. Yamada, C. Herrmann, G. Horn, H. R. Kalbitzer, K. Akasaka, *FEBS Lett.* **2001**, *506*, 180–184.
[13] A. Cooper, *Proc. Natl. Acad. Sci. USA* **1976**, *73*, 2740–2741.
[14] K. Akasaka, H. Li, *Biochemistry* **2001**, *40*, 8665–8671.
[15] Y. O. Kamatari, H. Yamada, K. Akasaka, J. A. Jones, C. M. Dobson, L. J. Smith, *Eur. J. Biochem.* **2001**, *268*, 1782–1793.
[16] W. Kremer, N. Kachel, K. Kuwata, K. Akasaka, H. R. Kalbitzer, *J. Biol. Chem.* **2007**, *282*, 22689–22698.
[17] a) A. Bundi, K. Wüthrich, *Biopolymers* **1979**, *18*, 285–297; b) D. S. Wishart, C. G. Bigam, A. Holm, R. S. Hodges, B. D. Sykes, *J. Biomol. NMR* **1995**, *5*, 67–81.

[18] M. R. Arnold, W. Kremer, H. D. Lüdemann, H. R. Kalbitzer, *Biophys. Chem.* **2002**, *96*, 129–140.
[19] J. Koehler, M. Beck Erlach, E. Crusca Jr., W. Kremer, C. E. Munte, H. R. Kalbitzer, *Materials* **2012**, *5*, 1774–1786.
[20] M. B. Erlach, J. Koehler, E. Crusca, Jr., W. Kremer, C. E. Munte, H. R. Kalbitzer, *J. Biomol. NMR* **2016**, *65*, 65–77.
[21] M. Beck Erlach, J. Koehler, E. Crusca, C. E. Munte, M. Kainosho, W. Kremer, H. R. Kalbitzer, *J. Biomol. NMR* **2017**, *69*, 53–67.
[22] M. Beck Erlach, J. Koehler, C. E. Munte, W. Kremer, E. Crusca, M. Kainosho, H. R. Kalbitzer, *J. Biomol. NMR* **2020**, *74*, 381–399.
[23] a) M. Beck Erlach, H. R. Kalbitzer, R. Winter, W. Kremer, *Biophys. Chem.* **2019**, *254*, 106239; b) C. E. Munte, M. Beck Erlach, W. Kremer, J. Koehler, H. R. Kalbitzer, *Angew. Chem. Int. Ed. Engl.* **2013**, *52*, 8943–8947; c) S. P. B. Vemulapalli, S. Becker, C. Griesinger, N. Rezaei-Ghaleh, *J. Phys. Chem. Lett.* **2021**, *12*, 9933–9939.
[24] S. Schwarzinger, G. J. A. Kroon, T. R. Foss, J. Chung, P. E. Wright, H. J. Dyson, *J. Am. Chem. Soc.* **2001**, *123*, 2970–2978.
[25] a) O. W. Howarth, D. M. J. Lilley, *Prog. Nucl. Magn. Reson. Spectrosc.* **1978**, *12*, 1–40; b) R. Richarz, K. Wüthrich, *Biopolymers* **1978**, *17*, 2133–2141.
[26] a) H. Schindelin, M. A. Marahiel, U. Heinemann, *Nature* **1993**, *364*, 164–168; b) A. Schnuchel, R. Wiltscheck, M. Czisch, M. Herrler, G. Willimsky, P. Graumann, M. A. Marahiel, T. A. Holak, *Nature* **1993**, *364*, 169–171.
[27] a) M. M. Garcia-Mira, D. Boehringer, F. X. Schmid, *J. Mol. Biol.* **2004**, *339*, 555–569; b) B. Köhn, M. Kovermann, *ChemBioChem* **2019**, *20*, 759–763; c) B. Köhn, M. Kovermann, *Nat. Commun.* **2020**, *11*, 5760; d) T. Schindler, M. Herrler, M. A. Marahiel, F. X. Schmid, *Nat. Struct. Biol.* **1995**, *2*, 663–673; e) T. Schindler, F. X. Schmid, *Biochemistry* **1996**, *35*, 16833–16842; f) M. Zeeb, J. Balbach, *J. Am. Chem. Soc.* **2005**, *127*, 13207–13212; g) M. Zeeb, M. H. Jacob, T. Schindler, J. Balbach, *J. Biomol. NMR* **2003**, *27*, 221–234.
[28] J. Roche, J. Ying, A. S. Maltsev, A. Bax, *ChemBioChem* **2013**, *14*, 1754–1761.
[29] D. S. Wishart, B. D. Sykes, *J. Biomol. NMR* **1994**, *4*, 171–180.
[30] L. Schrödinger, The PyMOL Molecular Graphics System, **2010**, *Version 2.5.0a0*.
[31] N. J. Baxter, M. P. Williamson, *J. Biomol. NMR* **1997**, *9*, 359–369.
[32] a) H. Schindelin, M. Herrler, G. Willimsky, M. A. Marahiel, U. Heinemann, *Proteins* **1992**, *14*, 120–124; b) M. Piotto, V. Saudek, V. Sklenár, *J. Biomol. NMR* **1992**, *2*, 661–665; c) M. Ikura, L. E. Kay, A. Bax, *Biochemistry* **1990**, *29*, 4659–4667; d) F. Delaglio, S. Grzesiek, G. W. Vuister, G. Zhu, J. Pfeifer, A. Bax, *J. Biomol. NMR* **1995**, *6*, 277–293; e) B. A. Johnson, R. A. Blevins, *J. Biomol. NMR* **1994**, *4*, 603–614; f) D. S. Wishart, C. G. Bigam, J. Yao, F. Abildgaard, H. J. Dyson, E. Oldfield, J. L. Markley, B. D. Sykes, *J. Biomol. NMR* **1995**, *6*, 135–140.

Manuscript received: January 19, 2024
Accepted manuscript online: April 24, 2024
Version of record online: June 4, 2024